New method for finding and characterizing WHIM structures

J. Nevalainen[1], M. Bonamente[2], E. Branchini[3], M. Einasto[1], A. Finoguenov[4], J. Liivamagi[1], P. Heinamaki[5], P. Nurmi[5], M . Roncarelli[6], A. Tamm[1], E. Tempel[1], E. Tilton[7], E. Saar[1]

1) Tartu Observatory
2) University of Alabama in Huntsville
3) University Roma Tre
4) University of Helsinki
5) Tuorla Observatory
6) Universita di Bologna
7) University of Colorado

IAU symposium 308, 23-28 June 2014 Tallinn, Estonia

PUT project funded by Estonian Research Council

http://www.aai.ee/~jukka/WBANG/WBANG_homepage.html

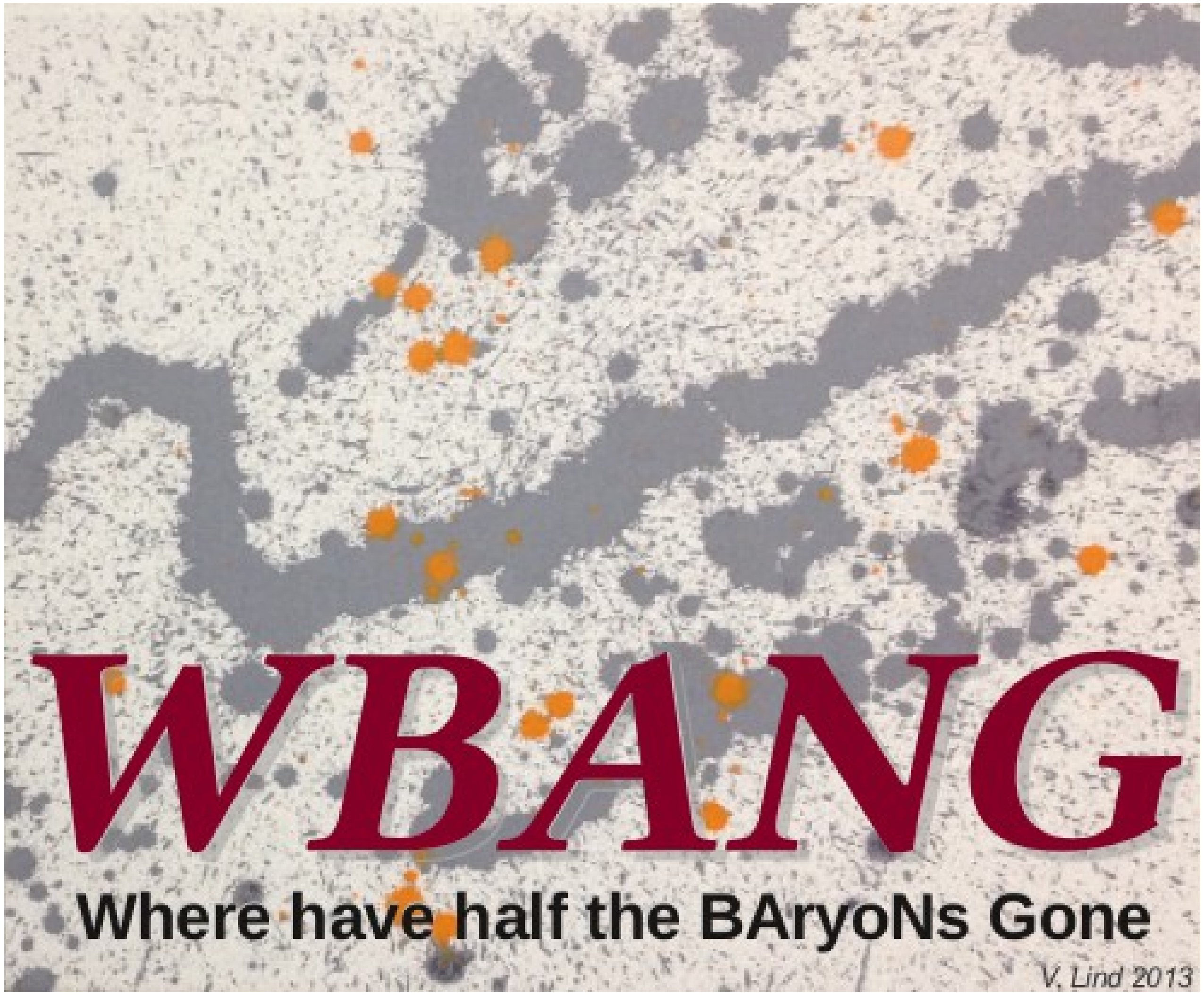

OUTLINE

Redshift < 0.2

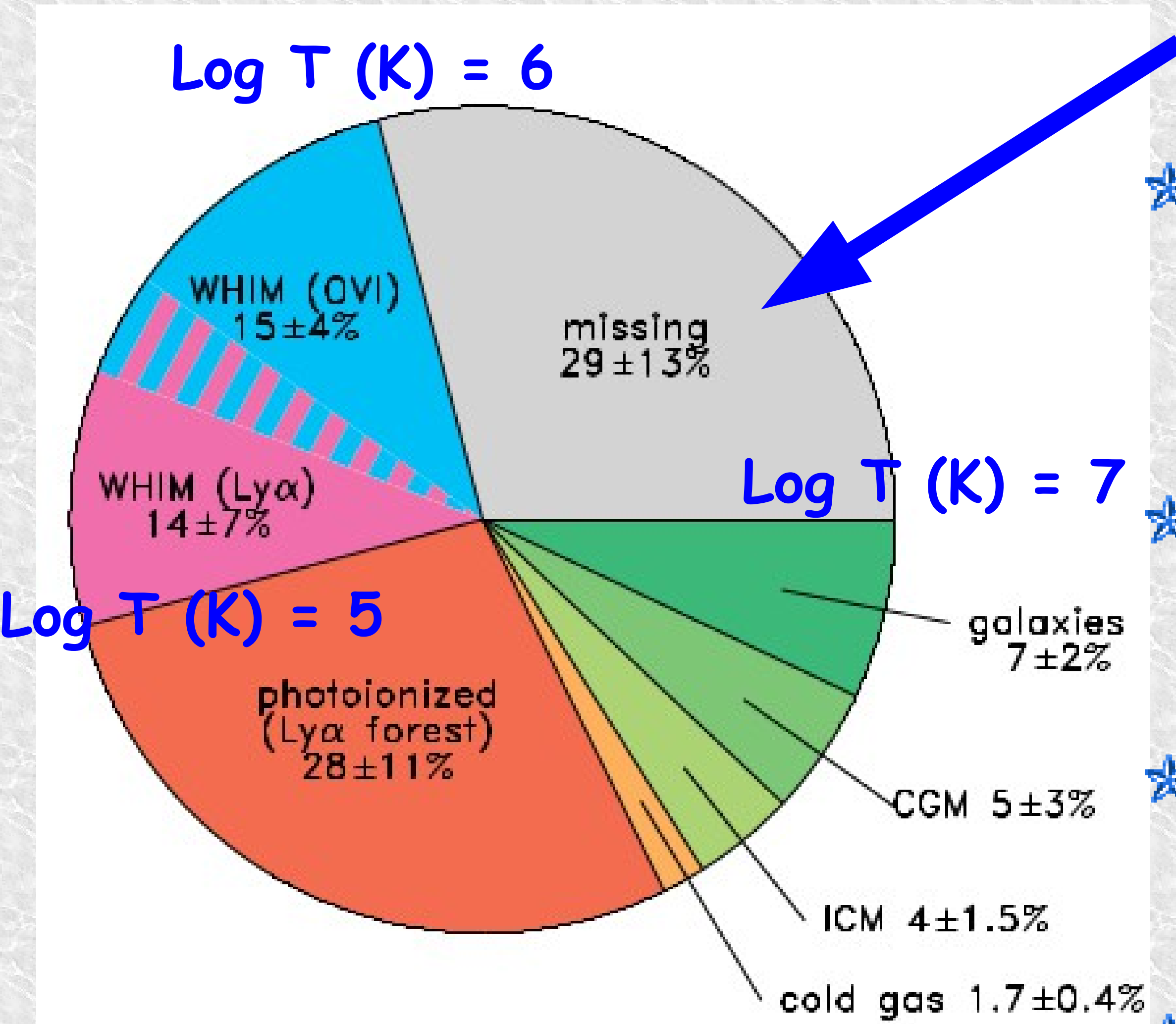

Shull et al., 2012, ApJ, 759, 23

- We look for the local missing baryons to complete the cosmological puzzle
- We assume the missing baryons are Warm Hot Intergalactic Medium within LSS galaxy filaments
- We aim at measuring WHIM redshifts, densities, temperatures and metallicities
- Results will help understand the thermal and chemical evolution of the local intergalactic medium
- Our method is based on a priori knowledge of galaxy structures, not blind search

1) Data

SDSS and 2DF

- We work with spectroscopic galaxy surveys
- Largest galaxy redshift survey available, Sloan Digital Sky Survey (SDSS) DR8
- Two-degree-field Galaxy Redshift Survey (2dF)
- 25% of the sky covered out to z=0.2

SDSS

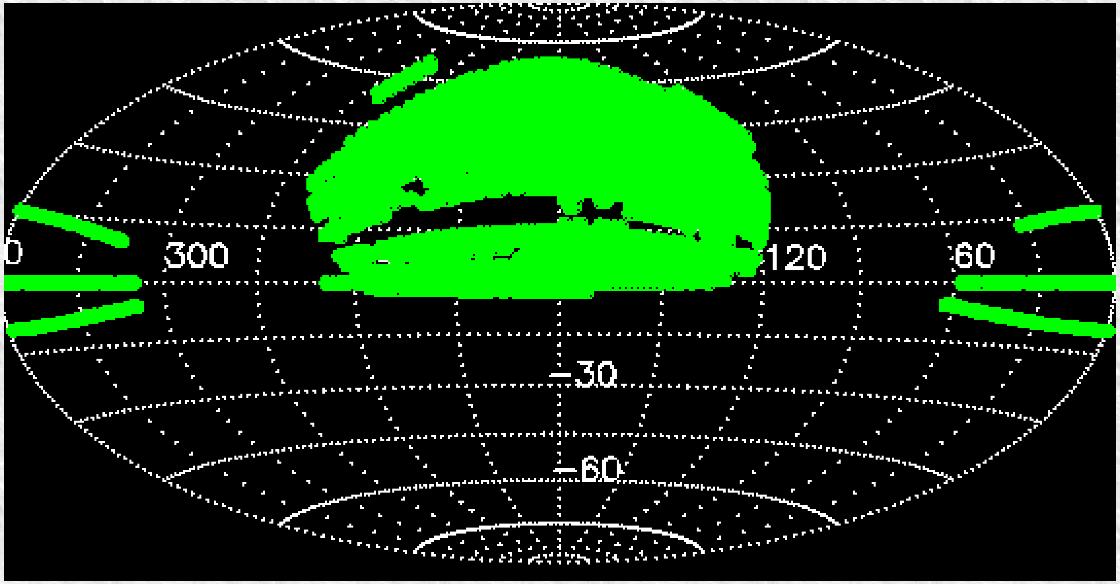

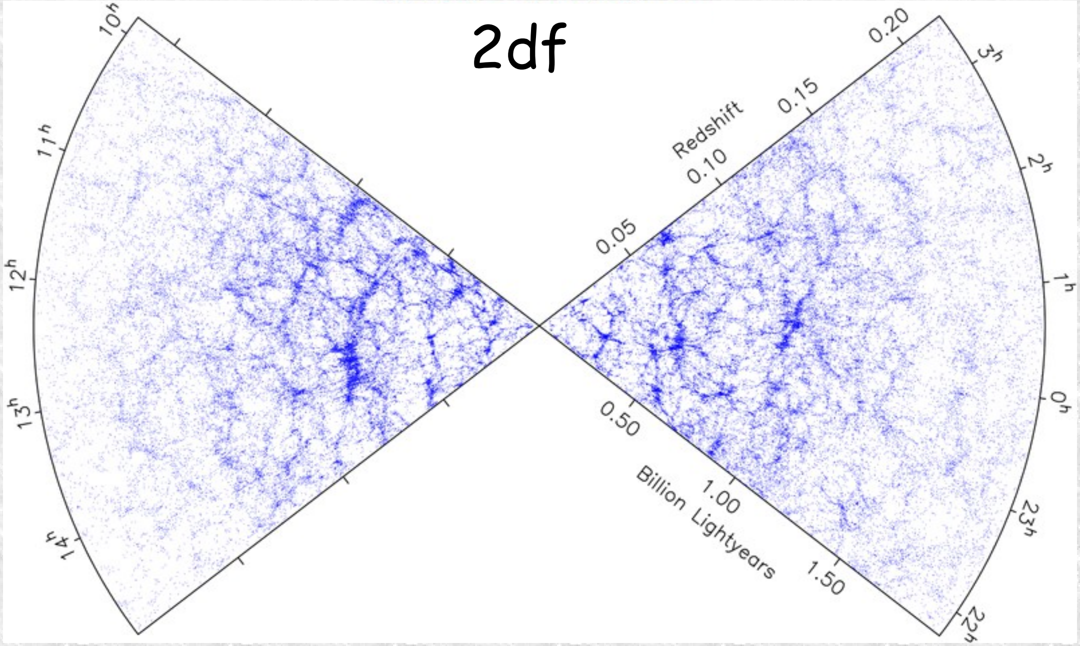

2) Identification of filaments

Filaments

- We assume that WHIM is located within the galaxy filaments connecting clusters and superclusters, as indicated by many simulations

- We apply object point process (Bisous process) to construct the filamentary galaxy network to SDSS and 2dF (E. Tempel's talk, E. Tempel 2014, MNRAS, 438, 3465)

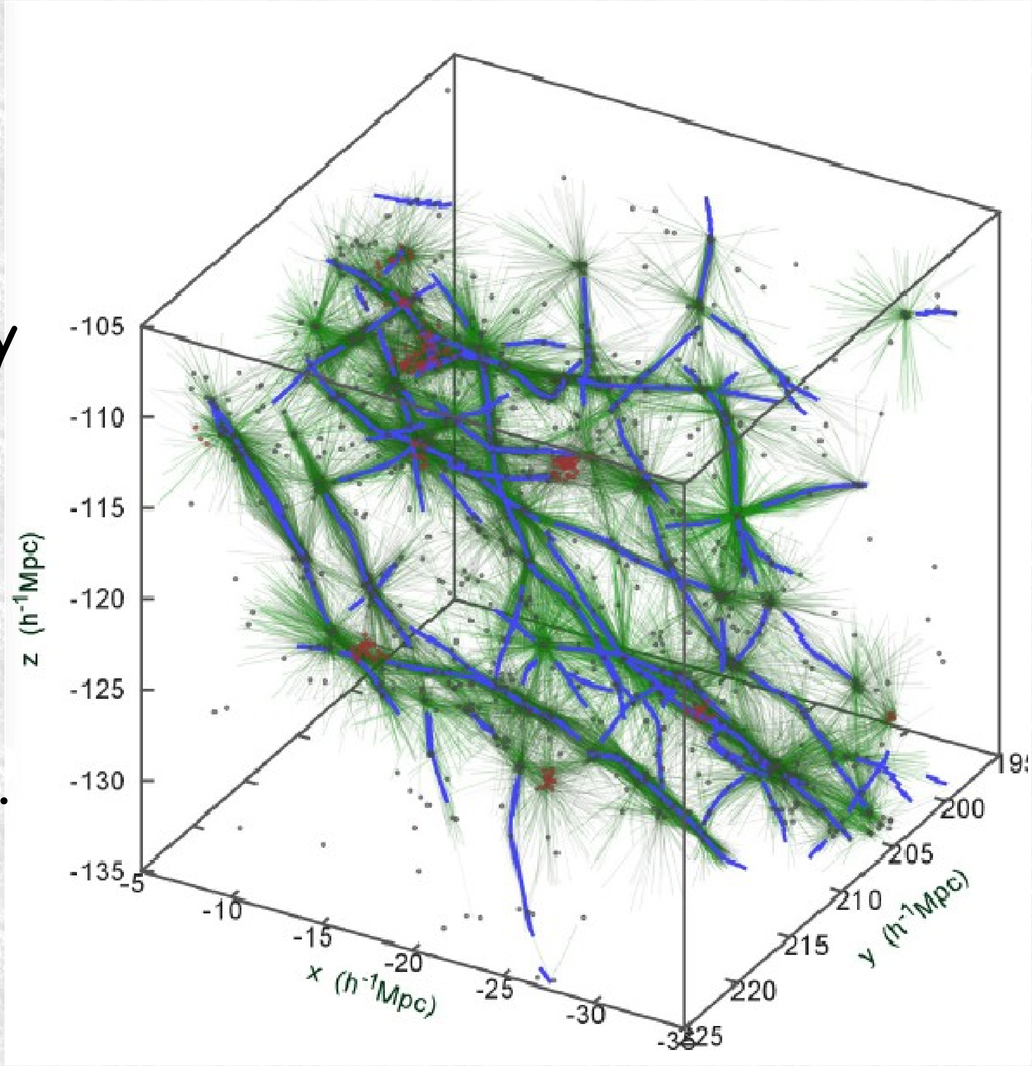

- Data base of potential WHIM locations and redshifts

Filament spines extracted from SDSS (Tempel et al, 2014, MNRAS, 438, 346)

3) Luminosity density fields as tracers of dark matter and thus of WHIM

LD fields

- We assume that galaxies follow the underlying dark matter potential, similarly as the WHIM
- 3D smoothing of the galaxy r-band luminosities yields the luminosity density field
- LD field yields the integrated LD in any line-of-sight to be used to estimate the WHIM N_H within any identified filamentary structure

Luminosity density field at a distance of 50 Mpc/h extracted from SDSS (Tempel et al, 2014, MNRAS, 438, 346)

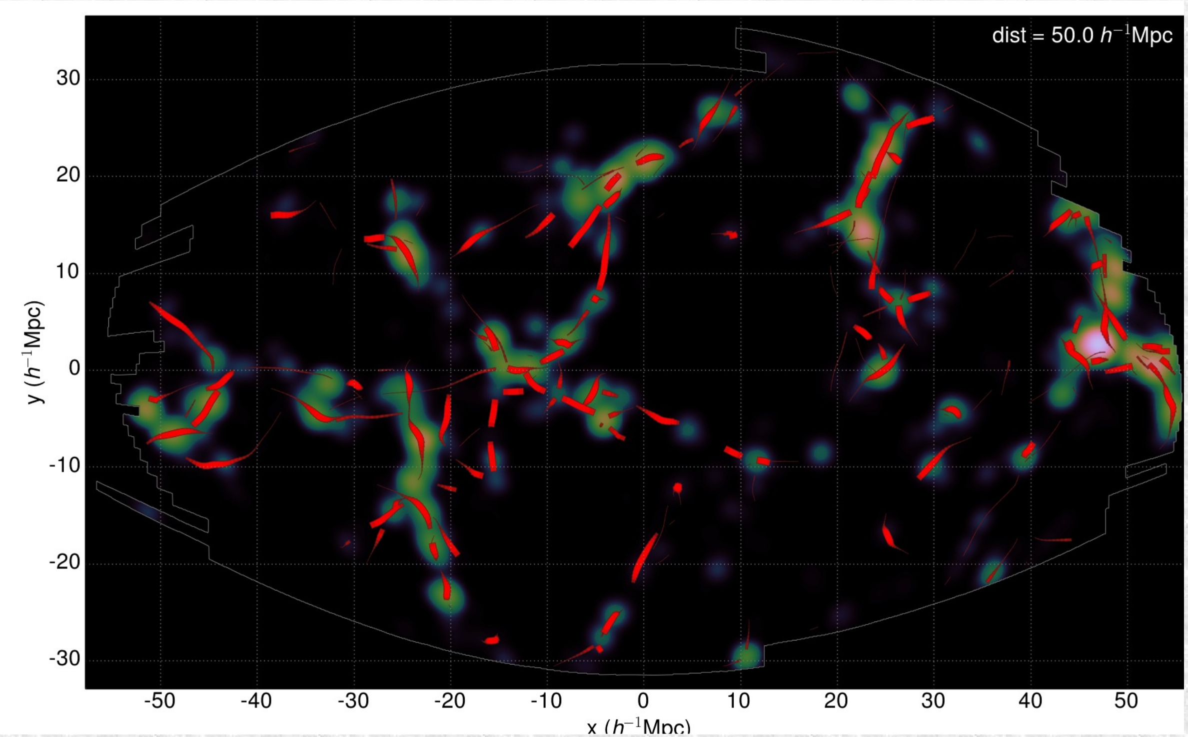

4) Simulations to link WHIM and LD (via DM)

- Cui et al. (2012) LSS SPH GADGET-3 simulations of DM and baryons
- Radiative cooling + star formation + kinetic feedback from SN
- $410^3\ h_{100}^{-3}\ \mathrm{Mpc}^3$ box
- DM resolution $4 \times 10^9\ M_\odot/h$
- Baryon resolution $7 \times 10^8\ M_\odot/h$

- DM haloes populated with galaxies using SDSS HOD (Zedavi+, 2011, ApJ, 736, 59)
- LD field created within $(1\ \mathrm{Mpc}/h)^3$ grid
- WHIM ≡ baryons with $T = 10^{5-7}$ K, mapped into $(1\ \mathrm{Mpc}/h)^3$ grid
- We then collect the WHIM densities in all such grid points where LD is within a given LD bin

Cui et al. (2012, MNRAS, 423, 2279)

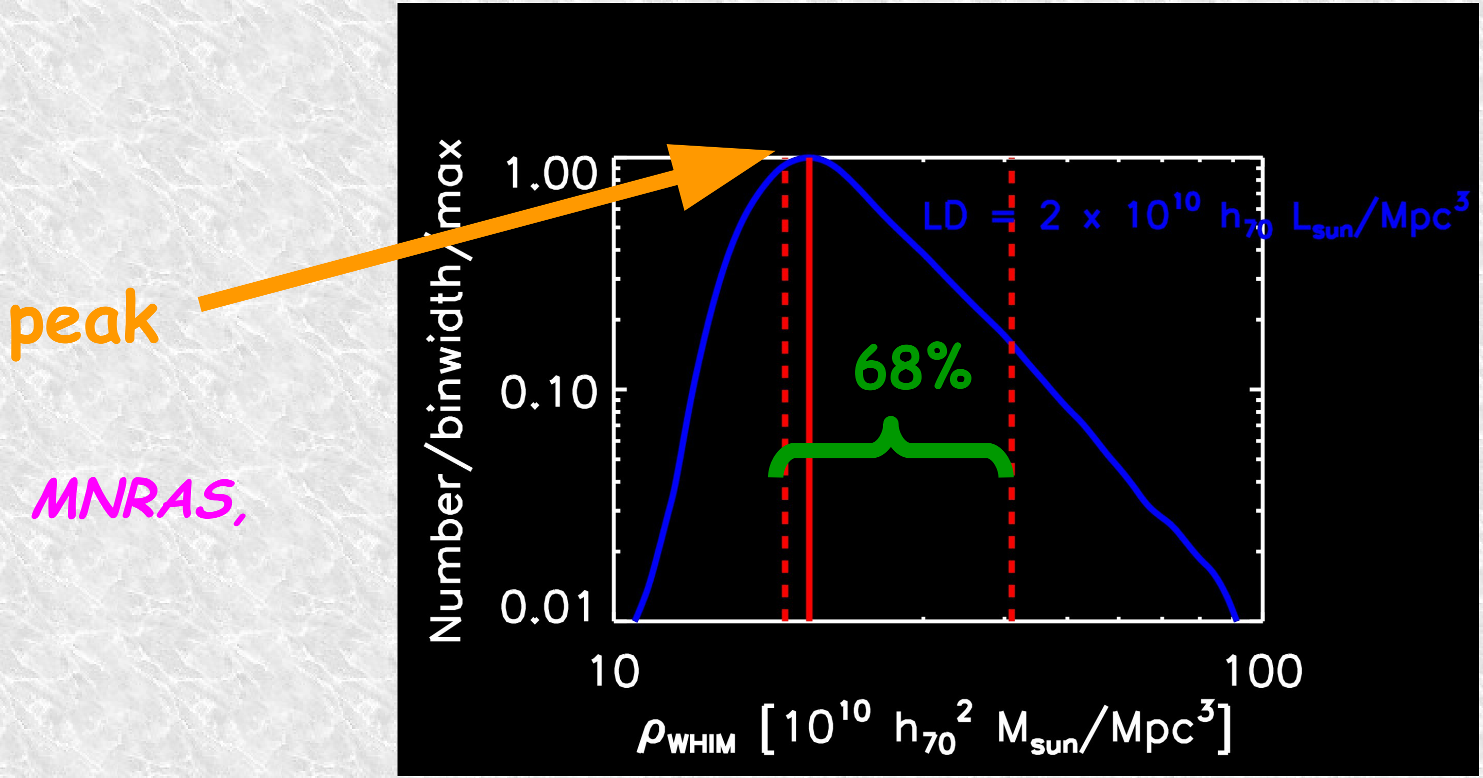

WHIM-LD relation $P(\rho_{WHIM} \mid LD_i)$

WHIM-LD rather linear in the δ_b = 1 - 10 range, as assumed

At highest LD sublinear: WHIM $\propto$ LD$^{\sim 0.8}$

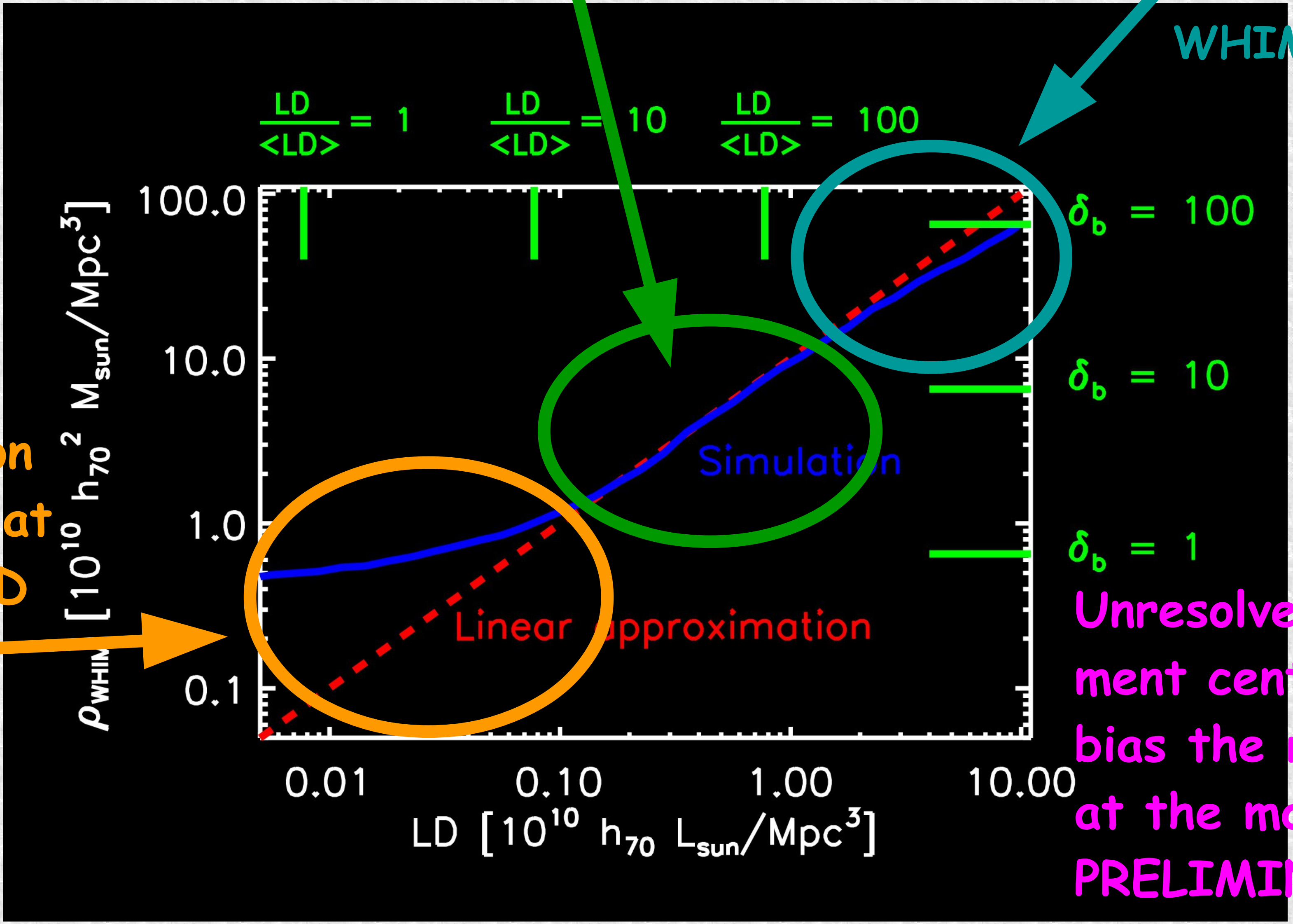

Resolution problem at lowest LD

Unresolved fila-ment centers may bias the relation at the moment. PRELIMINARY!

Uncertainty from the 68% scatter of WHIM at each LD

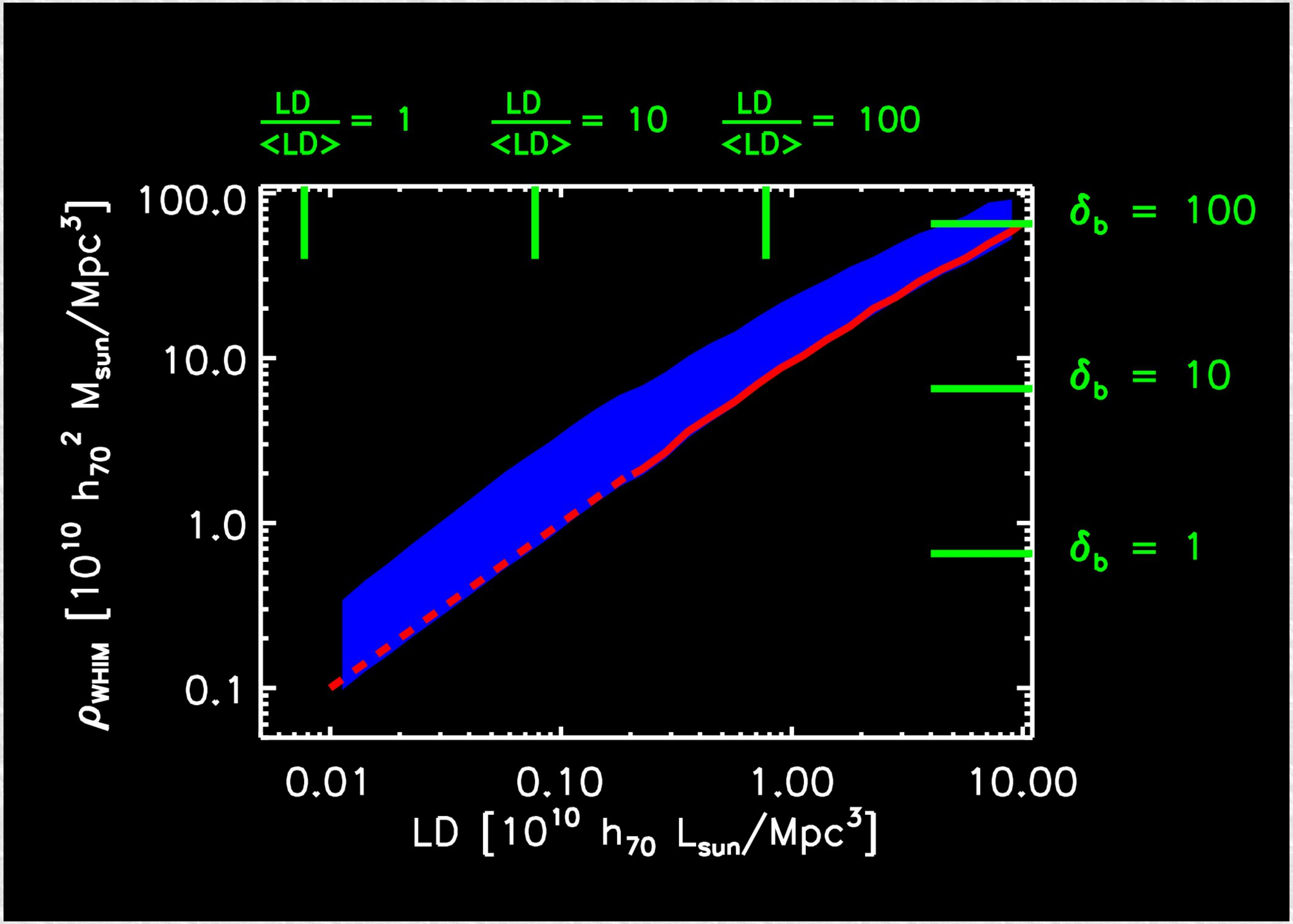

- asymmetric
- For a given LD, WHIM density estimate varies by a factor of 1.5 - 4.0 at 1σ

5) Testing the method with Sculptor

- The X-ray absorption lines of H2356-309 blazar behind Sculptor yielded redshifts and column densities for 3 WHIM structures (Fang et al., 2010, ApJ, 714, 1715; Zappacosta et al., 2010, ApJ, 717, 74)
- We will test how well our method will identify these structures and estimate the WHIM column density

Sculptor Wall z = 0.03

2dF data

O VII X-ray centroid, consistent with a significant galaxy structure

Fang et al., 2010, ApJ, 714, 1715

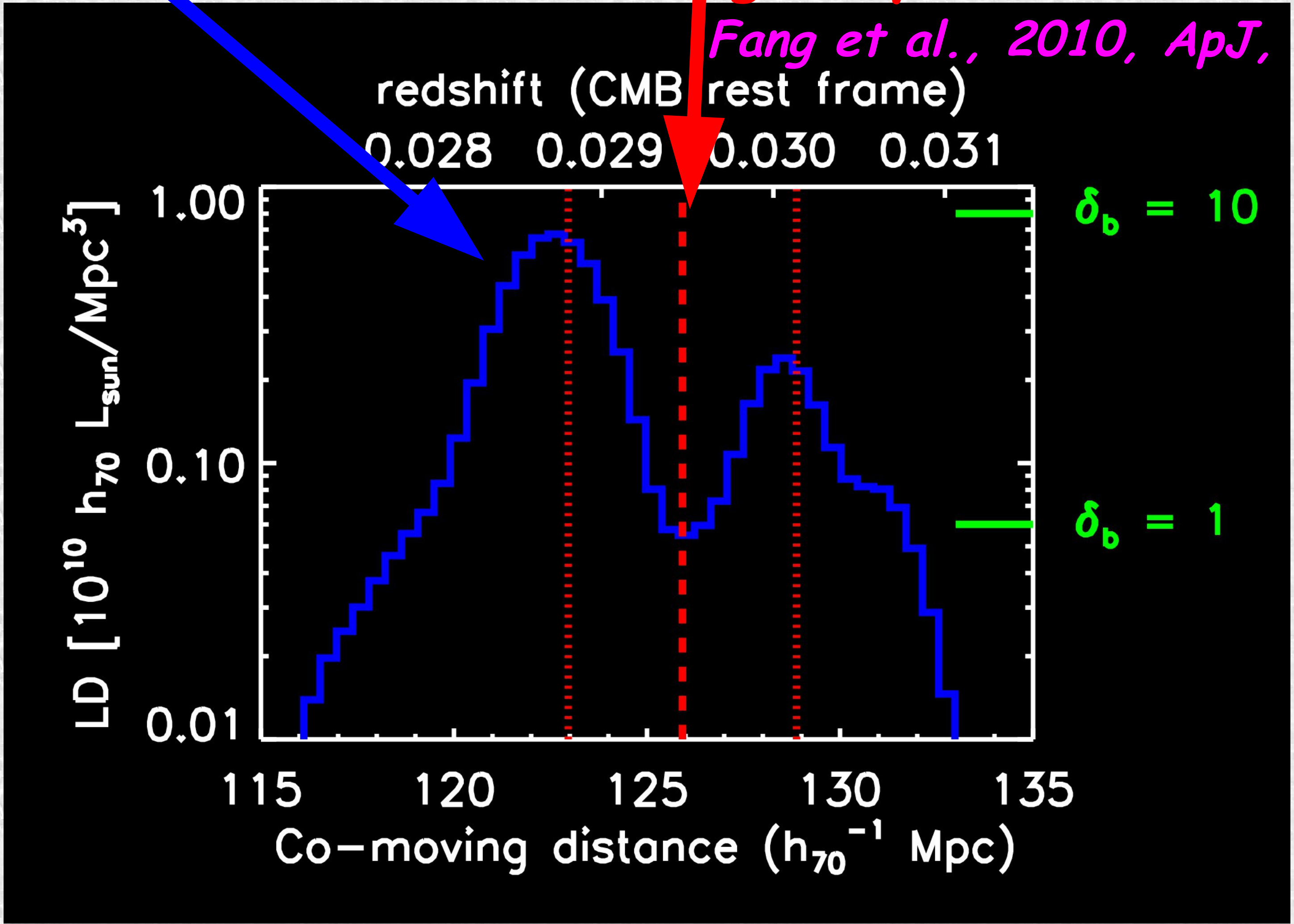

Sculptor Wall z = 0.03

Fang et al., 2010, ApJ, 714, 1715

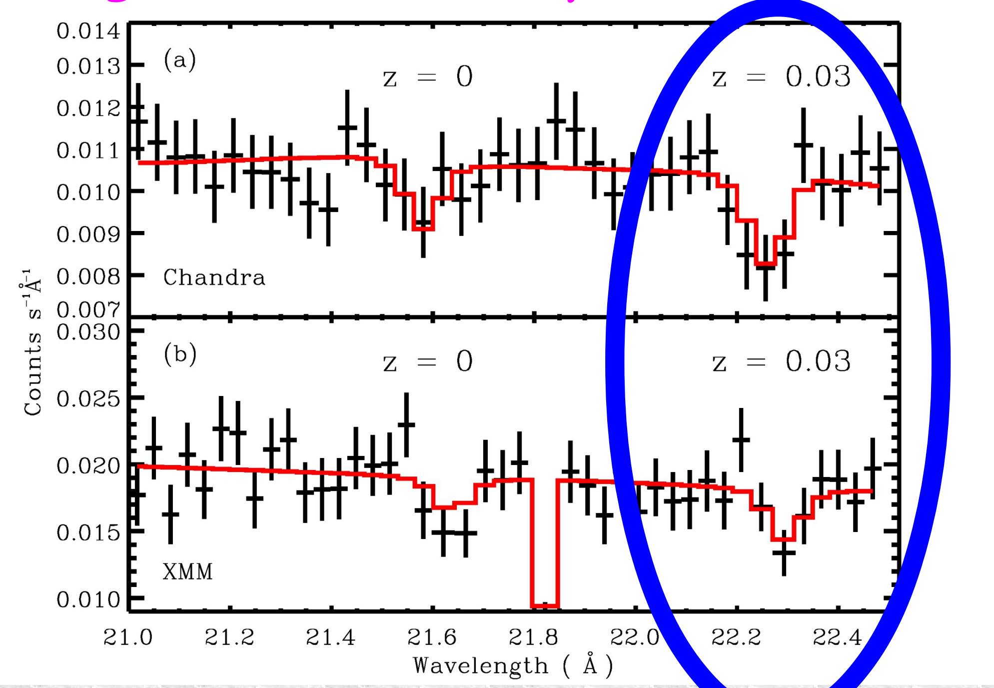

Log N_{OVII} (X-ray) = 16.9 (16.0 – 18.2)

$N_{OVII} = N_H \times f_{OVII} \times A_O \times (O/H)_\odot$

$T \equiv 10^6$ K ➔ f_{OVII} = 1.0

$A_O \equiv$ 0.1 solar

$(O/H)_\odot = 6.8 \times 10^{-4}$ (Grevesse et al., 1998, SSRv 85, 161) ➔

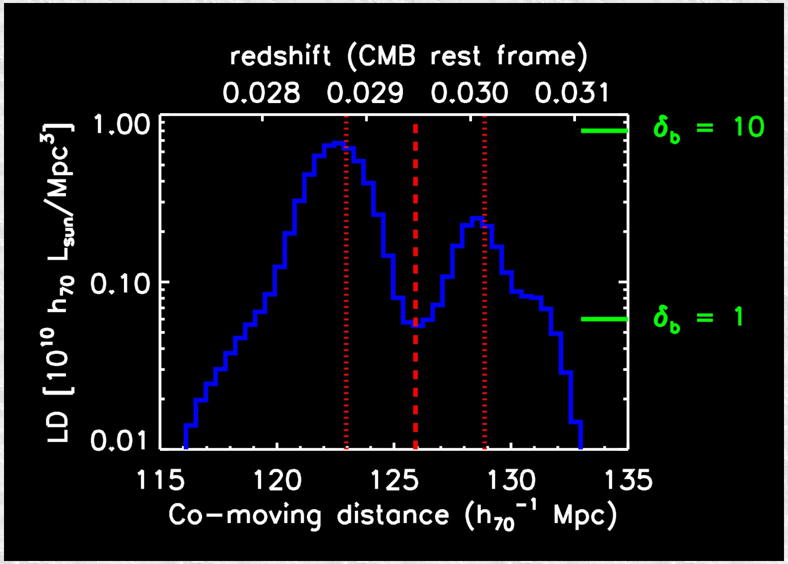

log N_H (X-ray) = 21.0 (20.1-22.2)

log N_H (LD) = 19.6 (19.6-20.1)

Consistent within large 1σ

Sculptor z = 0.06 (Pisces-Cetus)

2dF data

O VII X-ray centroid

Zappacosta et al., 2010, ApJ, 717, 74

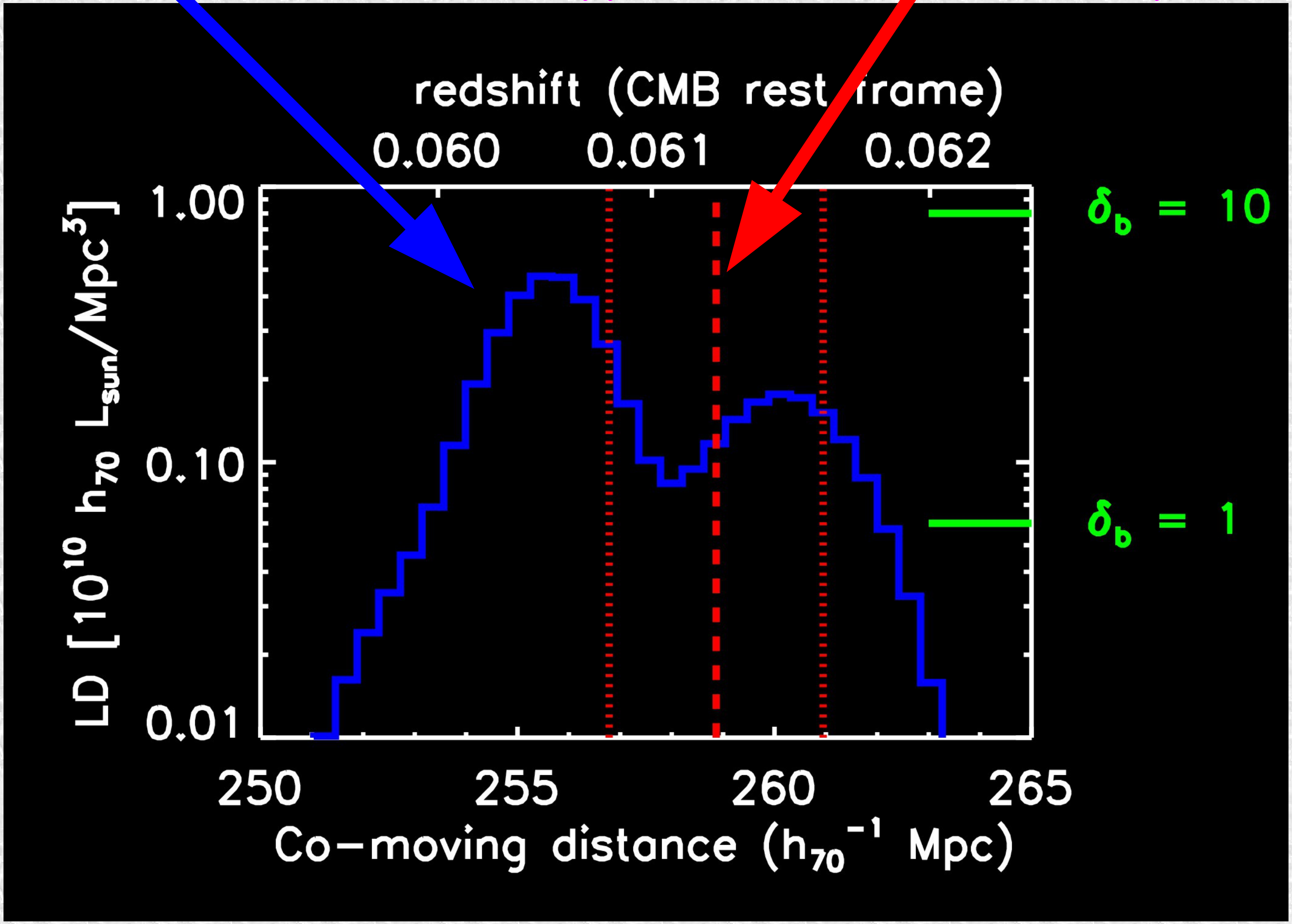

Sculptor z = 0.06 (Pisces-Cetus)

Zappacosta et al., 2010, ApJ, 717, 74

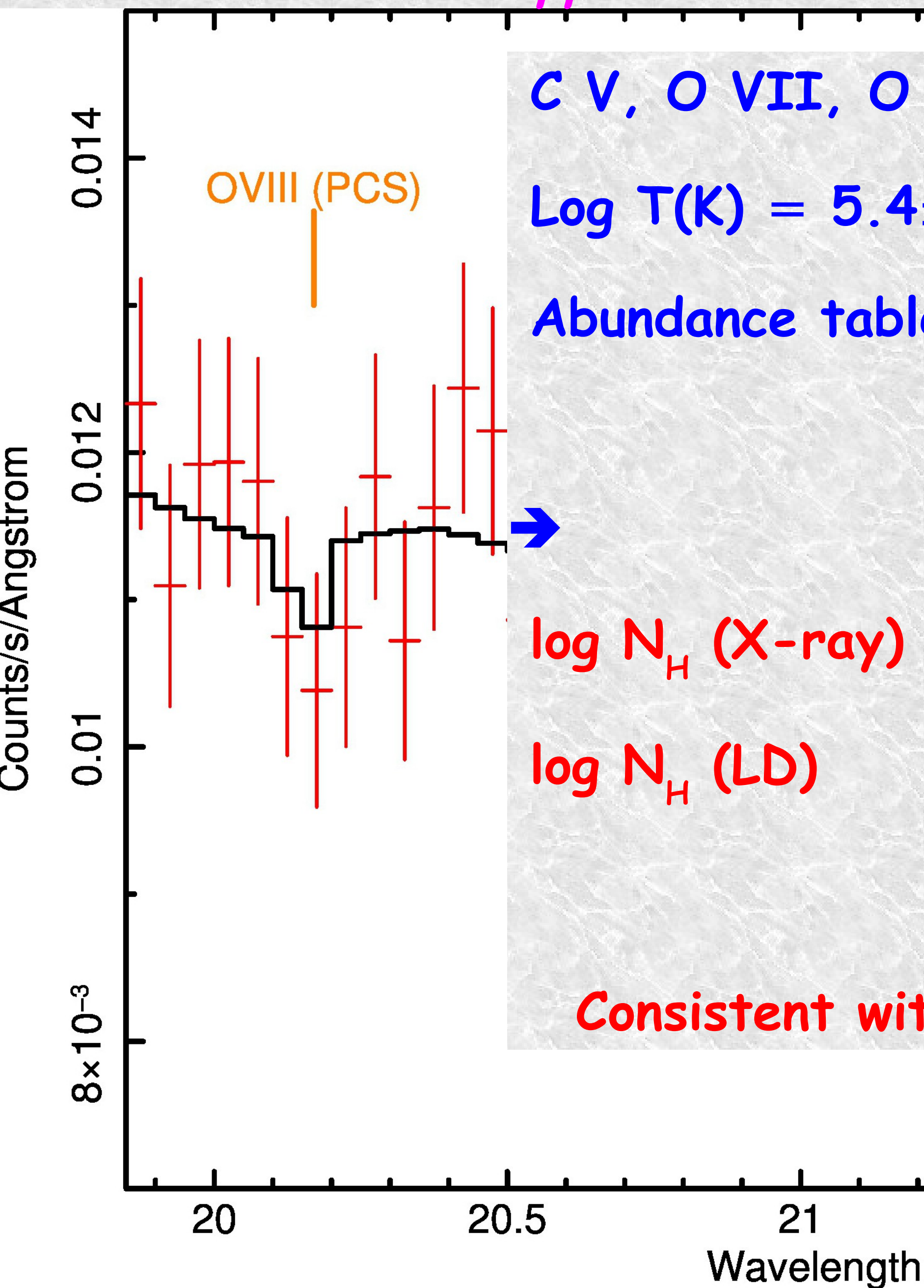

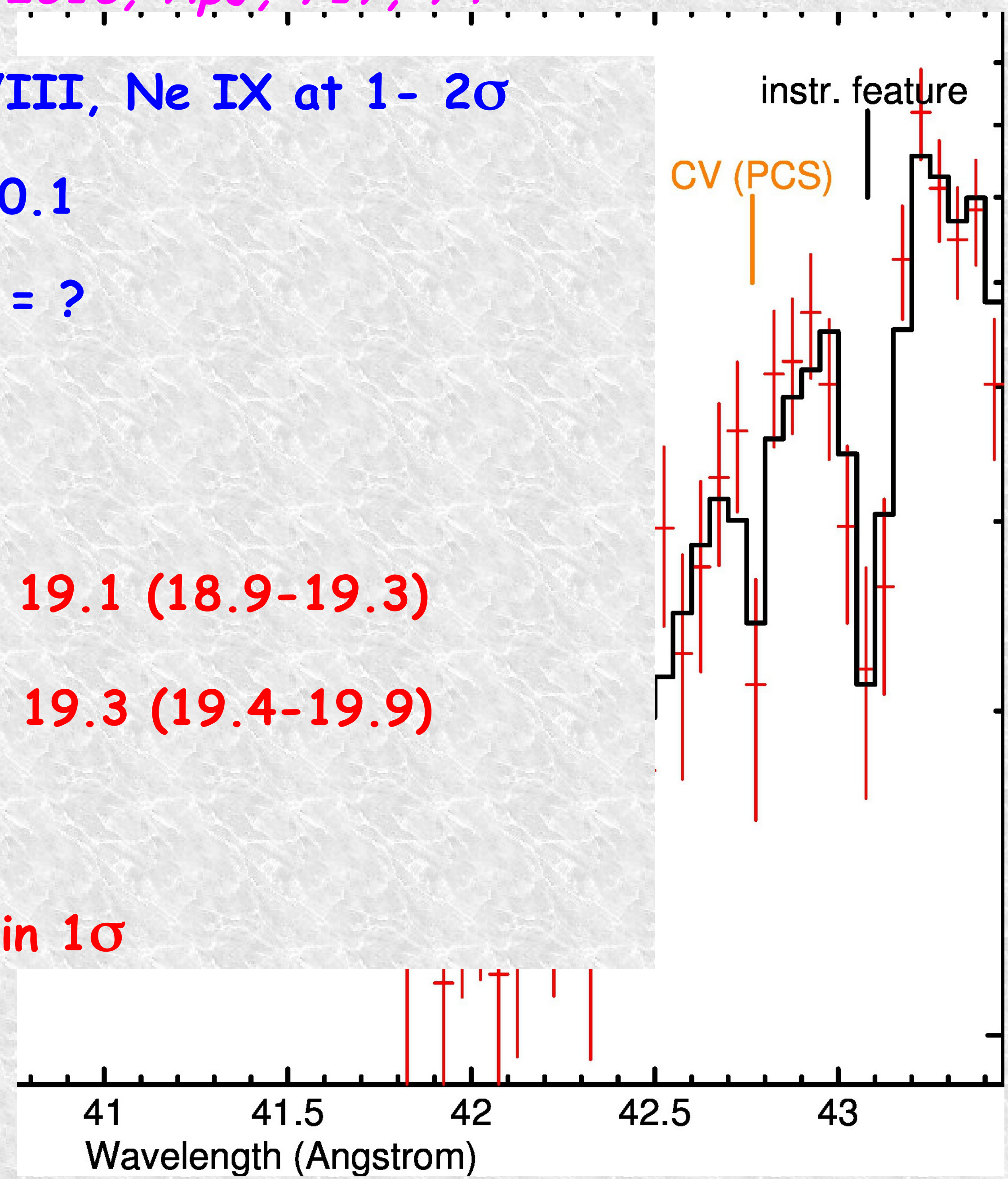

C V, O VII, O VIII, Ne IX at 1- 2σ

Log T(K) = 5.4$\pm$0.1

Abundance table = ?

➔

log N_H (X-ray) = 19.1 (18.9-19.3)

log N_H (LD) = 19.3 (19.4-19.9)

Consistent within 1σ

Farther Sculptor Wall z = 0.12

2dF data

O VII X-ray centroid

Zappacosta et al., 2010, ApJ, 717, 74

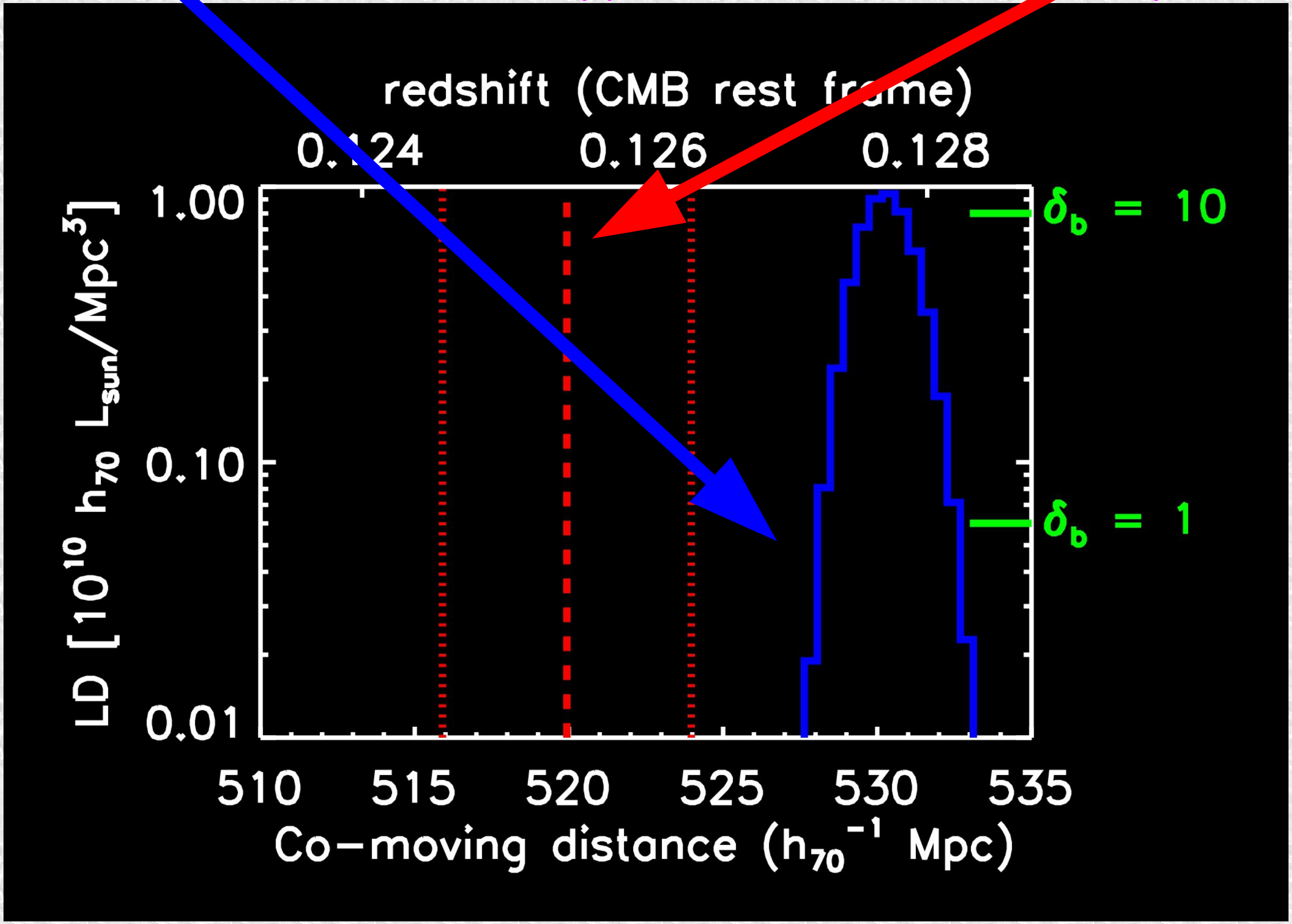

Farther Sculptor Wall z = 0.12

Zappacosta et al., 2010, ApJ, 717, 74

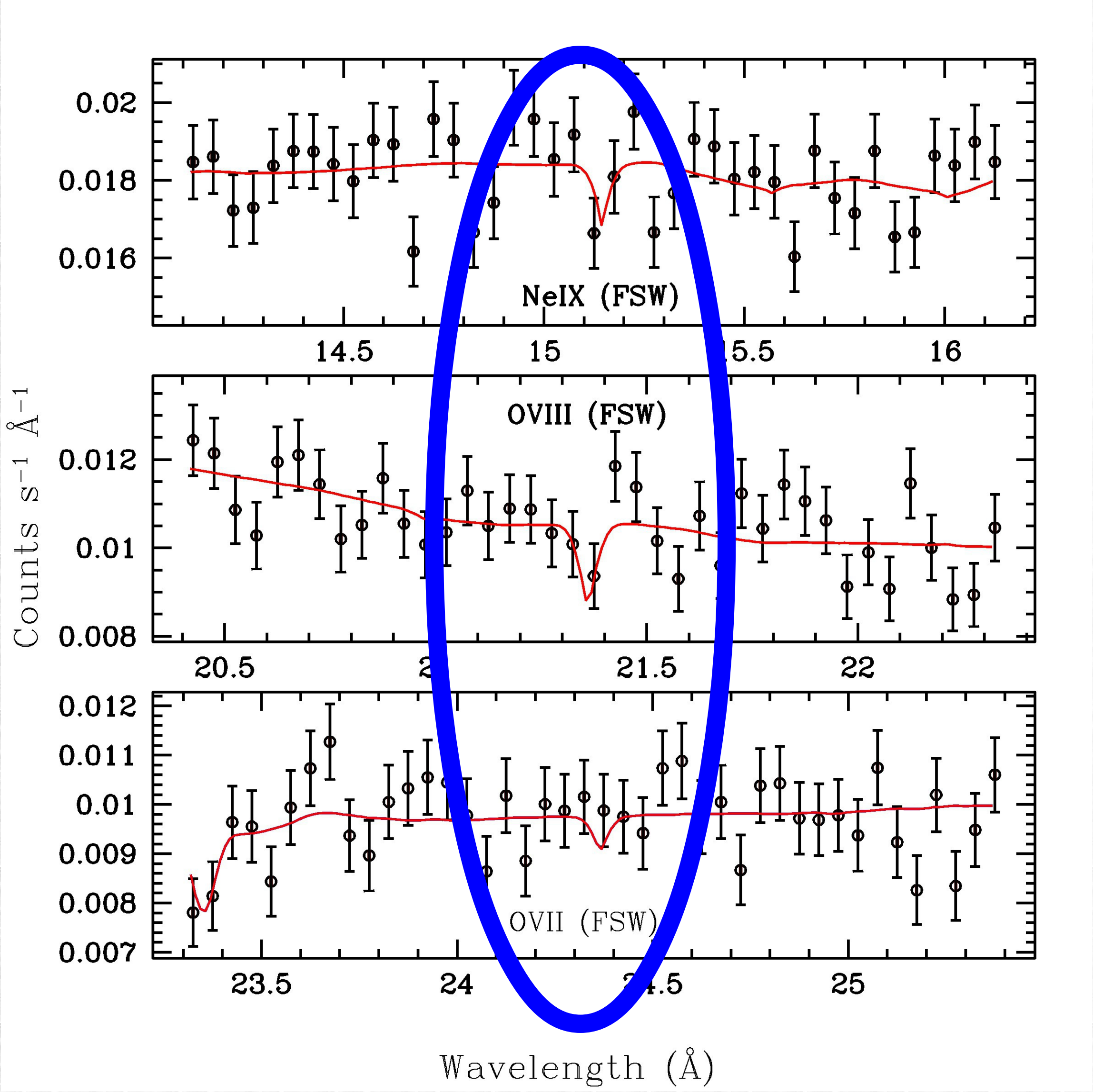

C VI, O VIII, Ne IX at 1- 2σ

Log T(K) = 6.6+0.1-0.2

Abundance table = ?

➔

log N_H (X-ray) = 19.8 (19.0-20.2)

log N_H (LD) = 19.4 (19.4-19.8)

Consistent at 1σ

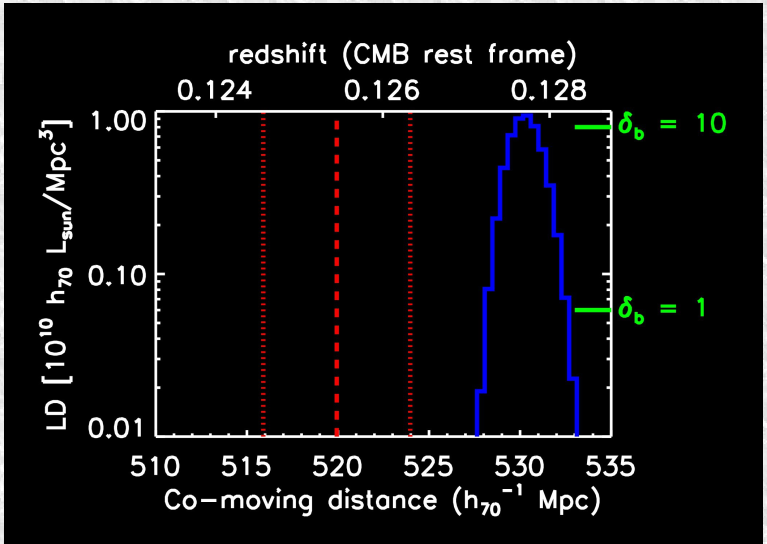

Summary of LD v.s. X-ray for Sculptor

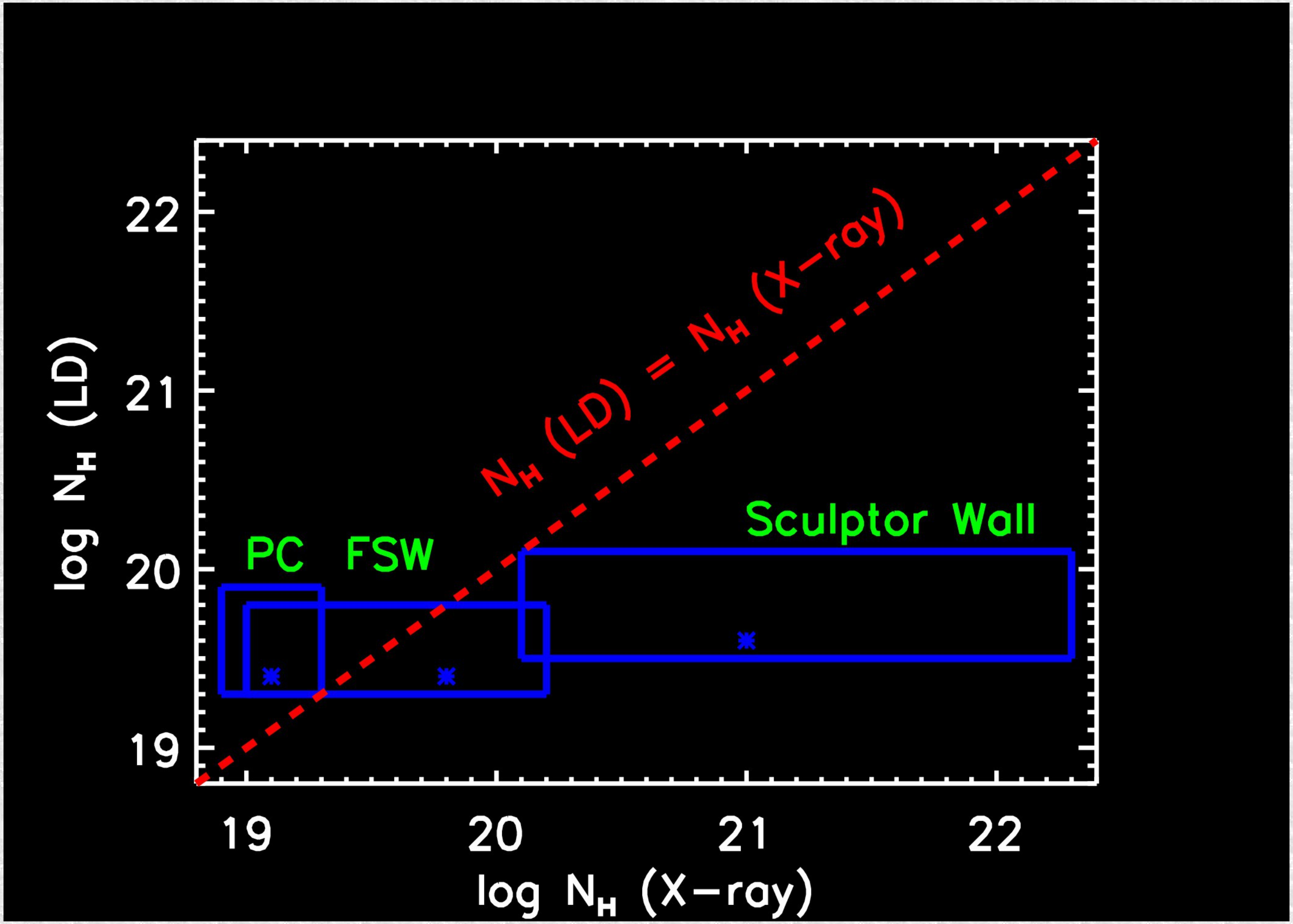

6) WHIM absorption line analysis of PKS 2155-304

PKS 2155-309 sightline

2dF luminosity density field
in 20x20x60 Mpc/h box

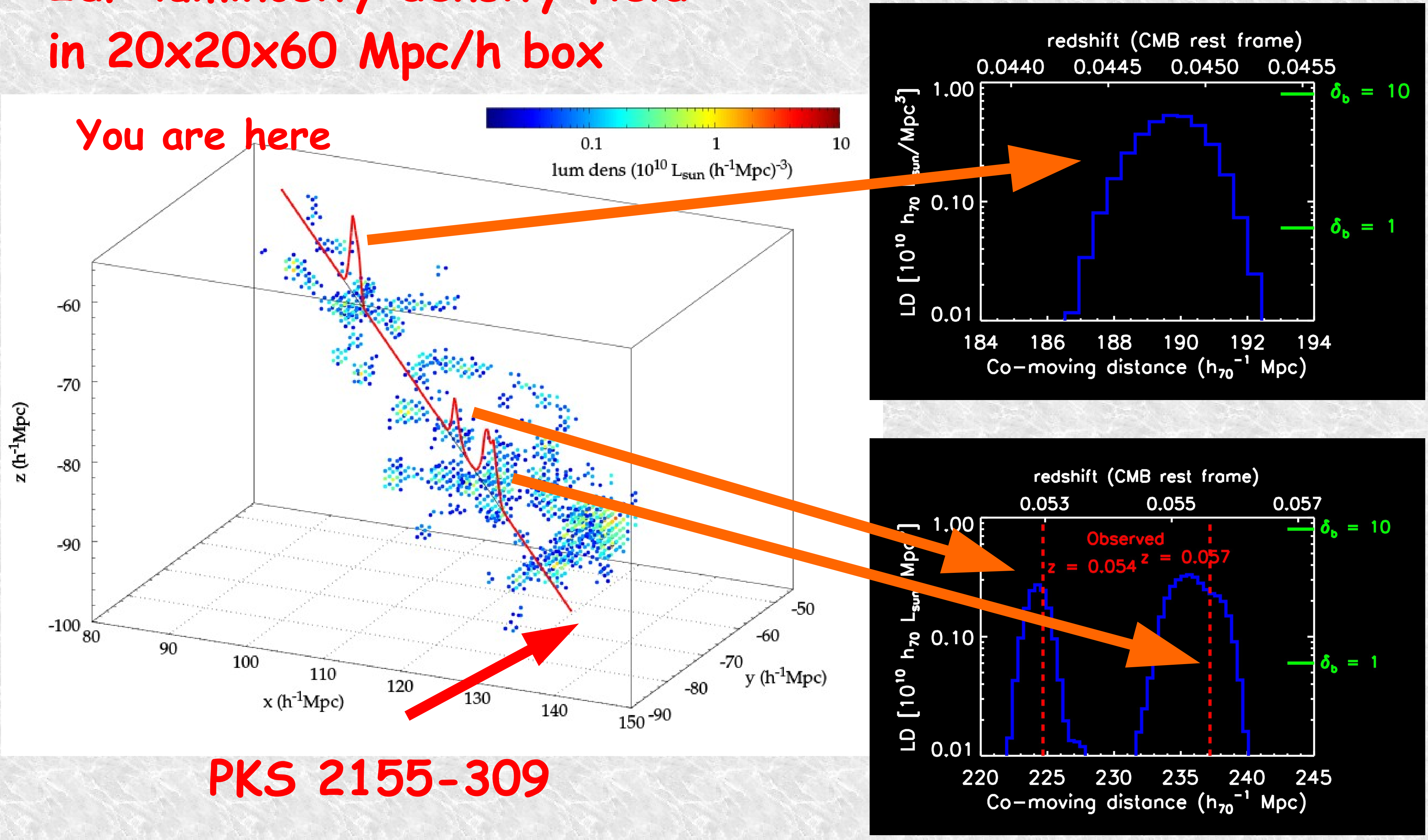

PKS 2155-309

PKS 2155-309 sightline

PKS 2155-304 OVI FUSE line

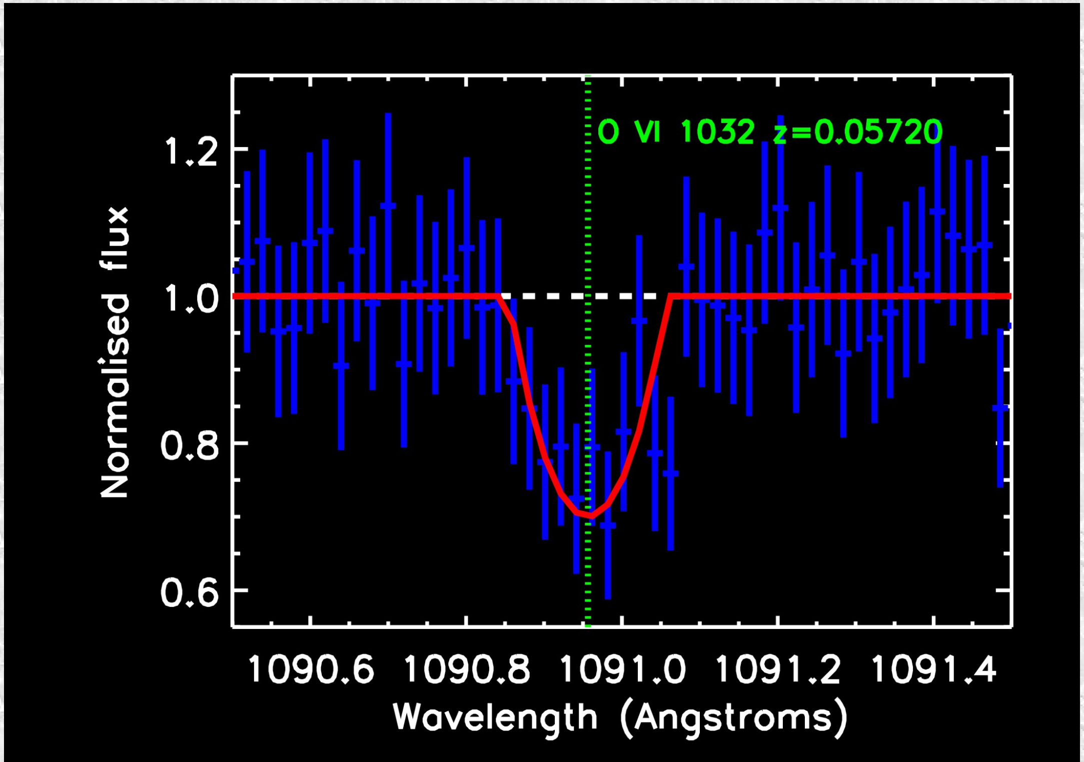

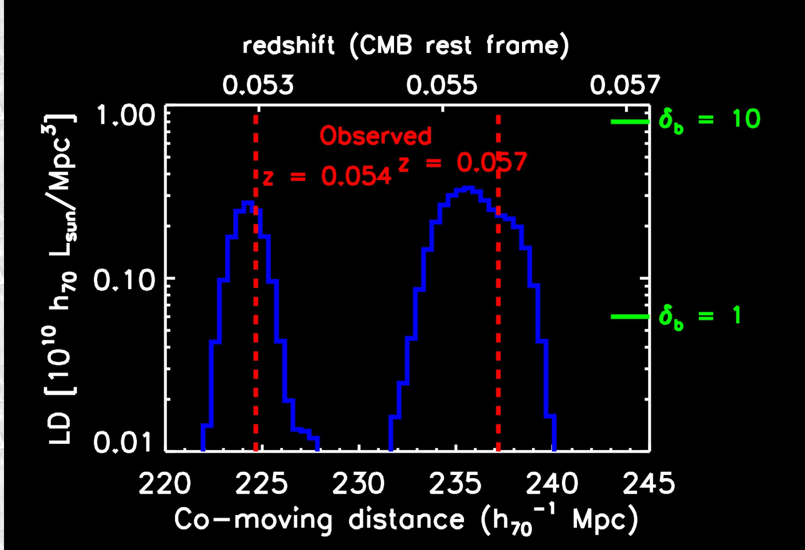

- 6σ detection of OVI absorption line with FUSE (Tilton et al., 2012, ApJ, 759, 112)
- Redshift matches the z = 0.057 2dF galaxy structure
- $N_{OVI} = 2.3 \pm 0.7 \times 10^{13}$ cm^{-2}
- Assuming the O VI line broadening is purely thermal, b = 24$\pm$7 km/s yields temperature constraint log T(K) = 5.7$\pm$0.3

Ionic fraction of O VI

LD method yields log N_H = 19.4 (19.3-19.9)

$N_{OVI} = N_H \times f_{OVI}(T) \times A_O \times (O/H)_\odot$ ➔

f_{ion} -T data from Mazzotta+ 1998

$F_{OVI} \geq 2 \times 10^{-3}$ (assuming a wide prior $A_O \leq$ 1.0 solar)

➔ **log T(K) = 5.2 - 6.3**

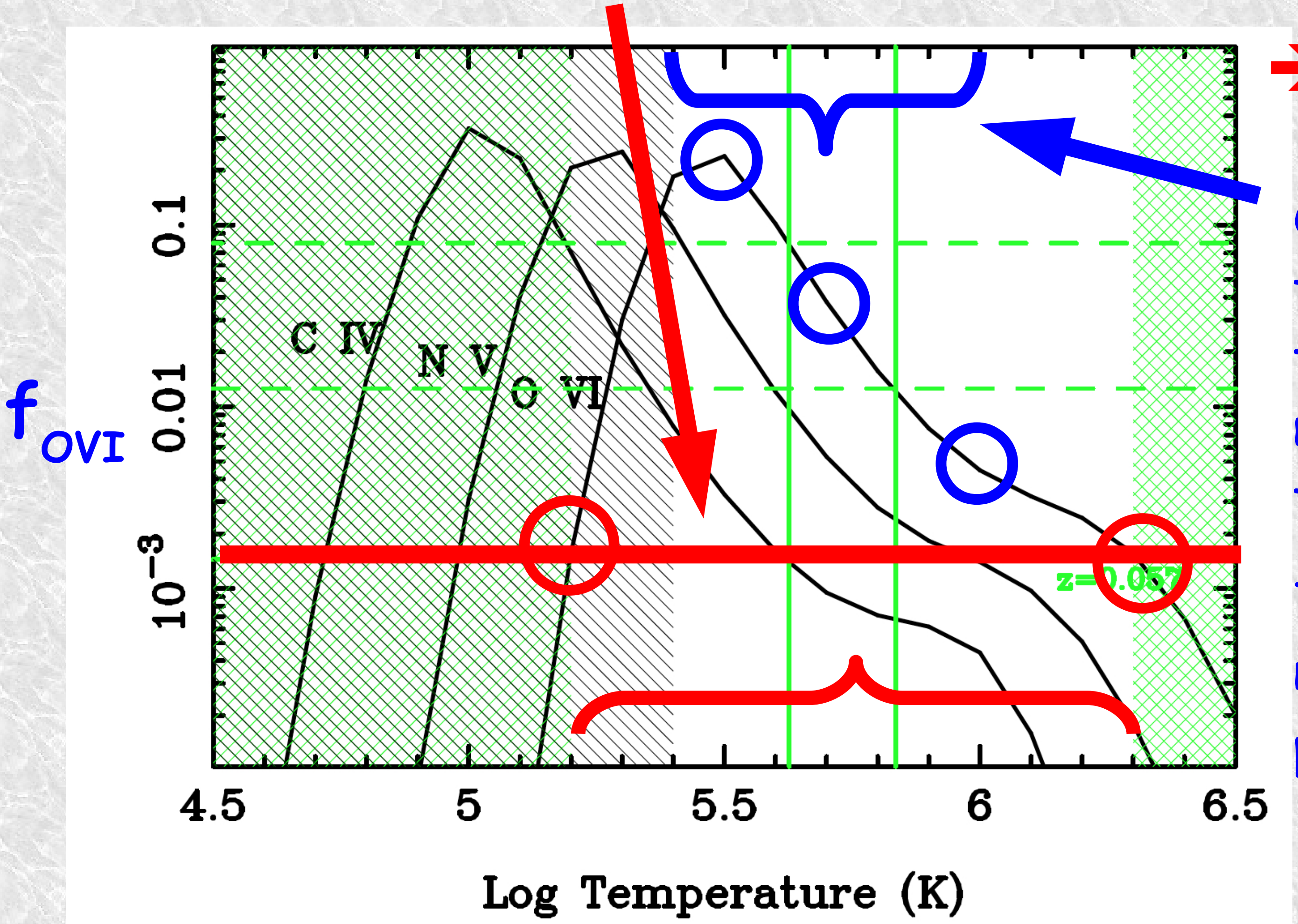

Our T constraint is consistent with that derived from thermal broadening. I.e. our method valid, and no non-thermal broadening.

Thermal O VI line broadening T constraint corresponds to

$$f_{OVI} = 4^{+16}_{-3.6} \times 10^{-2}$$

Oxygen abundance

- Combining OVI FUSE results for N OVI and f_{OVI} with our N_H estimate, we can derive constraints for the Oxygen abundance using:

$$N_{OVI} = N_H \times f_{OVI} \times A_O \times (O/H)_\odot$$

- This yields $A_O = 0.05 \pm 0.05$, i.e. observational constraint for the Oxygen abundance of WHIM using a single line, consistent with the simulations

FULL SDSS

- Filaments from full SDSS **DONE** (Tempel+ 2014)
- LD fields
- WHIM densities ➔ large WHIM data base
- For high enough N_{WHIM}, cross-correlation with bright enough blazars
- We use MAXI all sky X-ray monitor for triggering so that we catch the blazar flare in the early phase ➔
  we can extend the data base of blazars used for WHIM absorption towards fainter and more distant ones ➔
  extension of WHIM absorption detection data base for cosmological studies

Summary

- Method based on 2dF and SDSS spectroscopic galaxy catalogues
- Identification of filaments using Bisous model (Tempel+ 2014)
- Luminosity density LD fields around the identified filaments as a tracer of dark matter and thus WHIM
- Large scale simulations for relation btw. WHIM and LD
- Method yields filament locations, sizes, redshifts and WHIM N_H
- N_H agrees with X-ray absorption estimates in Sculptor
- Additional WHIM NH constraint improves the absorption line diagnostics